Nano Energy 122 (2024) 109289

Contents lists available at ScienceDirect

Nano Energy

journal homepage: www.elsevier.com/locate/nanoen

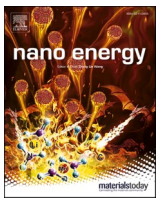

Full paper

Controllable and large-scale synthesis of carbon quantum dots for efficient solid-state optical devices

Weihua Li [a], Xiaohan Wang [a,*], Jishuai Lin [a], Xiangyong Meng [a], Lihua Wang [a], Maorong Wang [a], Qiang Jing [a], Yang Song [a], Alberto Vomiero [b,c,**], Haiguang Zhao [a,*]

[a] College of Textiles and Clothes, State Key Laboratory of Bio-Fibers and Eco-Textiles, College of Physics, University Industry Joint Center for Ocean Observation and Broadband Communication, Qingdao University, No. 308 Ningxia Road, Qingdao 266071, PR China
[b] Department of Molecular Sciences and Nanosystems, Ca' Foscari University of Venice Via Torino 155, 30172 Venezia Mestre, Italy
[c] Department of Engineering Sciences and Mathematics, Luleå University of Technology, 97187 Luleå, Sweden

ARTICLE INFO

Keywords:
Carbon quantum dots
Foam structure
Microwave reaction
Anti-counterfeiting
Luminescent solar concentrators

ABSTRACT

Carbon quantum dots (C-dots) showed excellent structure-tunable optical properties, mainly composed of carbon, nitrogen and oxygen. They have been used for various types of solid-state optical devices. Due to the photoluminescence quenching caused by aggregation, it is a challenge to produce high quantum yield and large Stokes shift C-dots via controllable and simple approaches. In this work, we demonstrated a microwave assisted heating approach for the high-quality C-dots production with ten grams scale per batch in less than 4 min. The addition of metal cation promoted the formation of the foam-structure by forming carboxyl-metal-amine complex, enabling the spatial confined growth of the C-dots in a solid-state, contributing to the high quantum yield (QY) of 73% with a Stokes shift of 0.65 eV. By tuning the structure of the C-dots, excitation dependent and independent photoluminescent (PL) behavior were achieved because of the formation of the different types of energy states evidenced by transient PL and femtosecond transient absorption spectroscopy. These optical properties enable the C-dots to be successfully integrated in luminescent solar concentrators (LSCs), having an external optical efficiency of 3.0% and a power conversion efficiency of 1.3% (225 cm^2) and an excitation-dependent high-level anticounterfeiting fluorescent code, showing a great potential for solid-state optical system.

1. Introduction

Quantum dots are semiconductor nanocrystals, showing size-tunable optical properties because of quantum confinement [1]. Differently from quantum dots, Carbon quantum dots (C-dots) are composed of carbon, nitrogen, and oxygen, without containing heavy-metals [2–4]. The optical properties of C-dots are determined by both core structure and their functional surface groups, which offers facile solution to tune their functional properties [3,4]. C-dots have been widely used for various types of optoelectronic devices, including luminescent solar concentrators (LSCs), fluorescent anticounterfeiting code, light-emitting diodes (LEDs), catalysis, biomedical sensors and so on, because of their low-cost, easy synthesis and tunable optical and electrical properties [3–15]. The key factors still required for these devices applications is to obtain C-dots, having structure-tunable absorption/emission, high quantum yields (QYs), with single/multiple photoluminescent (PL) peak and large Stokes shift to avoid the energy reabsorption loss in specific applications like LSCs. To date, the blue and green emitting C-dots have the QYs exceeding 90% and the red-emitting C-dots have the QY of 70% [6,13,16]. For example, Yuan et al. reported the C-dots having the QY of 96% and Stokes shift of 0.3 eV, while their emission and absorption spectra showed a significant overlap [13]. It is still a challenge to keep the high QYs of the C-dots, meanwhile having a large Stokes shift or small absorption/emission spectral overlap, which plays an important role for large-scale solid-state optical applications [17].

C-dots have been produced via many approaches, including solvothermal/hydrothermal reaction, microwave-assisted reaction, vacuum heating, radical-assisted synthesis and so on [5,8,12,13,18–20]. Among these methods, microwave heating endows the simple and efficient production of the C-dots in a reaction time as short as several minutes [5,10,21,22]. The C-dots produced via microwave heating have the typical QY up to 99% for blue color C-dots, however, the obtained

* Corresponding authors.
** Corresponding author at: Department of Molecular Sciences and Nanosystems, Ca' Foscari University of Venice Via Torino 155, 30172 Venezia Mestre, Italy.
E-mail addresses: xh_wang@qdu.edu.cn (X. Wang), alberto.vomiero@ltu.se (A. Vomiero), hgzhao@qdu.edu.cn (H. Zhao).

https://doi.org/10.1016/j.nanoen.2024.109289
Received 13 December 2023; Received in revised form 9 January 2024; Accepted 10 January 2024
Available online 13 January 2024

QY is still less than 60% for green colored C-dots with several exception [5,9,20]. For example, Wei et al. reported the C-dots with QY of 75.9% via microwave heating approach in only 3 min with a reaction yield close to 70% [19]. However, in their synthesis, they used strong base NaOH and the PL and absorption spectra were largely overlapped with a Stokes shift of only 0.25 eV [19]. Zhou reported the synthesis of C-dots using a spatially confined vacuum heating approach, and they reported a QY as high as 70% using citric acid (CA) and urea as precursors, and $CaCl_2$ as dehydration and foaming agent [23]. Because of the reaction in the solid-state, and the growth of the C-dots confined by the space diffusion, the reaction time was as long as 2–3 h [8,18,23]. For the potential commercial use of the C-dots for various types of solid-optical devices, it is very important to develop a fast, cost-effective, and efficient approach for high quality C-dots.

In this study, we combined the microwave reaction and spatial-confined reaction and demonstrated a microwave assisted method to produce ten-gram-scale C-dots with multiple emissions, high QYs and large Stokes shift for anticounterfeiting and LSCs. With the fast reaction between the CA and $CaCl_2$, a foam structure formed in less than 10 s and confined the growth of the C-dots. By controlling the reaction time and the types of cations, we can produce the C-dots with excitation-dependent PL and excitation-independent PL behavior. The C-dots synthesized via optimized conditions have the QY as high as 73% with a Stokes shift of 0.65 eV. Benefiting from these properties, the as-prepared C-dots can be used as building blocks for making excitation-dependent fluorescent security code and large-area LSCs (225 cm^2) with a power conversion efficiency (PCE) of 1.3% under natural sunlight (50 mA/cm^2), showing a great potential for solid-state optical devices.

2. Experimental section

2.1. Synthesis of C-dots

Microwave reactor was used to produce C-dots. For a typical reaction, 10 g of CA and 10 g urea were mixed with 10 g of $CaCl_2$ in 20 mL water. The mixture was put inside the microwave with the powder of 700 W. The reaction was maintained for 2 min, 4 min and 6 min, and the as-prepared C-dots were defined as C-dots (2 M, 4 M and 6 M), respectively.

For a comparison, we also synthesized C-dots without adding $CaCl_2$, but keeping the same amount of CA and urea. After 2 min reaction, a brown color solid was formed without any foam. Different cations were used to produce the C-dots without changing the reaction parameters, but replacing the $CaCl_2$ with $AlCl_3$, $MgCl_2$, $SrCl_2$, $BaCl_2$, $MnCl_2$, and NaCl. We also produced the C-dots by tuning the mass ratio of the CA/urea/$CaCl_2$, for example (1:2:1).

Two-step approach was used to produce the C-dots. In details, the obtained C-dots by microwave after 2 min reaction using CA/urea/$CaCl_2$ was transferred to oven. The powder was heated to 200 ℃ for 3 h.

For all the obtained C-dots powder, they were dispersed in methanol/ethanol and filtered by a sieve. The mixture was further centrifuged at 8000 r.p.m. for 10 min. The supernatant was purified by using chromatographic silica columns, followed a dialysis process (3000 Da). The details were included in the supporting information (SI).

2.2. Ink printing

The fluorescent ink (3.5 mg/mL) was prepared by mixing 0.35 g blue-emitting C-dots (2 M) or green-emitting C-dots (4 M) powder with 100 mL of ethanol. The mixture was stirred at 8000 rate per minutes for 4 h and then filtered by 250 nm Millipore for 3 times. The non-fluorescent paper was pre-treated using polyvinyl alcohol (PVA) solution (2%) and after that the designed code was printed on the paper via Canon TS3480 printer. The earth and LSC in the florescent code were printed using the C-dots (2 M) based ink and the leaf in the florescent code was printed using the C-dots (4 M) based ink.

2.3. LSC preparation and optical characterizations

A film structured LSC was fabricated by a drop-casting approach. In details, the as-obtained C-dots powder (60 mg) was dispersed in the 30 mL polyvinyl pyrrolidone (PVP) solution (200 mg/mL). The mixture was stirred for 10 min to dissolve thoroughly, and centrifuged at 10,000 rate per minutes for 5 min to remove bubbles. Finally, the obtained mixture without aggregations or bubbles was drop-casted on glass (15 ×15 ×0.75 cm^3). After naturally drying the mixture for 4 h, a thin film with measured thickness of ~500 μm was obtained.

For the LSC measurements, one edge of the LSC was fully covered by the commercial solar cells (PCE: 15%). The optical efficiency and PCE of the LSCs were measured in ambient conditions at 18 ℃ (October, Qingdao, China). We chose the noon for the measurement with the light intensity of 50 mW/cm^2. The sunlight intensity was measured by using a calibrated Zolix QE-B1 solar cell. As the LSC is symmetrical, we can reasonably assume that the output fluorescent intensity at each edge is same. A power meter (Newport 843-R) was attached at the edge of the LSC for the measurement of the fluorescent light intensity. For the PCE measurement, the measured current intensity was used to calculate the PCE of the LSC by using the equation of $PCE = 4 \times (J_{sc} \times V_{oc} \times FF)/(P_{in} \times G) \times 100\%$. The geometric factor (G) was defined as the ratio of surface area and edge area (L/4d), where L is length of the LSC and d is the overall thickness of the LSC. In this study, the G factor is calculated as 4.7. The photostability of the LSC was measured by home-made set-up. The UV light with intensity of 100 mW/cm^2, was used to excite the LSC and the detector was put on the edge of the LSC in ambient conditions (25 ℃, 40% humidity). Other characterizations were included in the S.I.

3. Results and discussion

3.1. Synthesis and structure of the C-dots

Microwave assisted heating is a very efficient approach to produce nanocrystals as the electromagnetic wave can induce the molecular motion and mutual friction, converting electromagnetic energy into thermal energy, leading to the increase of the reaction temperature [24]. Typically, the microwave heating has several advantages, such as fast heating speed and high heating efficiency, and energy-saving. This explains the fast preparation of the C-dots using this approach. For the aqueous system, the reaction temperature was limited to 100 ℃ at ambient conditions, without using the autoclave. Thus, it is very difficult to prepare the highly carbonized C-dots at ambient conditions. Inspired by the vacuum heating approach reported by Zhou et al. [23] we used the microwave reactor to heat the mixture of CA/urea/metal cation, and we found a foam-structure formed in less than 10 s by the fast temperature increase rate of 6 ℃/second. This solid-state foam enables the further increase of the reaction temperature to 200 ℃ for the efficient carbonization under space-confinement growth. We investigated the formation mechanism for the foam-structure under microwave irradiation. Without using the metal cation, the CA and urea underwent a very fast reaction, and formed the brown solid in less than 4 min and without forming any foam structure (Fig. S1a, b). Using the monovalent metal cation, we observed the foam during the heating, while the foam cannot maintain its structure, with further heating, and the hard brown solid was achieved (Fig. S2). In a big contrast, by adding the bivalent or trivalent metal cations (e.g. Ca^{2+}, Mg^{2+}, Sr^{2+}, Ba^{2+}, Mn^{2+} and Al^{3+}), we are able to observe the foam structure with the volumetric expansion ratio over 10 times (Fig. 1b and Fig. S3). For example, for the CA-urea-Ca^{2+}, after 1.5 min heating, a white foam was obtained (Fig. 1b). After 2 min heating, a slightly yellow foam was achieved (Fig. 1c), due to the formation of the C-dots. After 4 min heating, a yellow-green powder was found with a clear green color upon illumination at 365 nm, because of the formation for the C-dots (Fig. 1d). We can produce the C-dots in ten-gram-scale per batch by simply scaling up

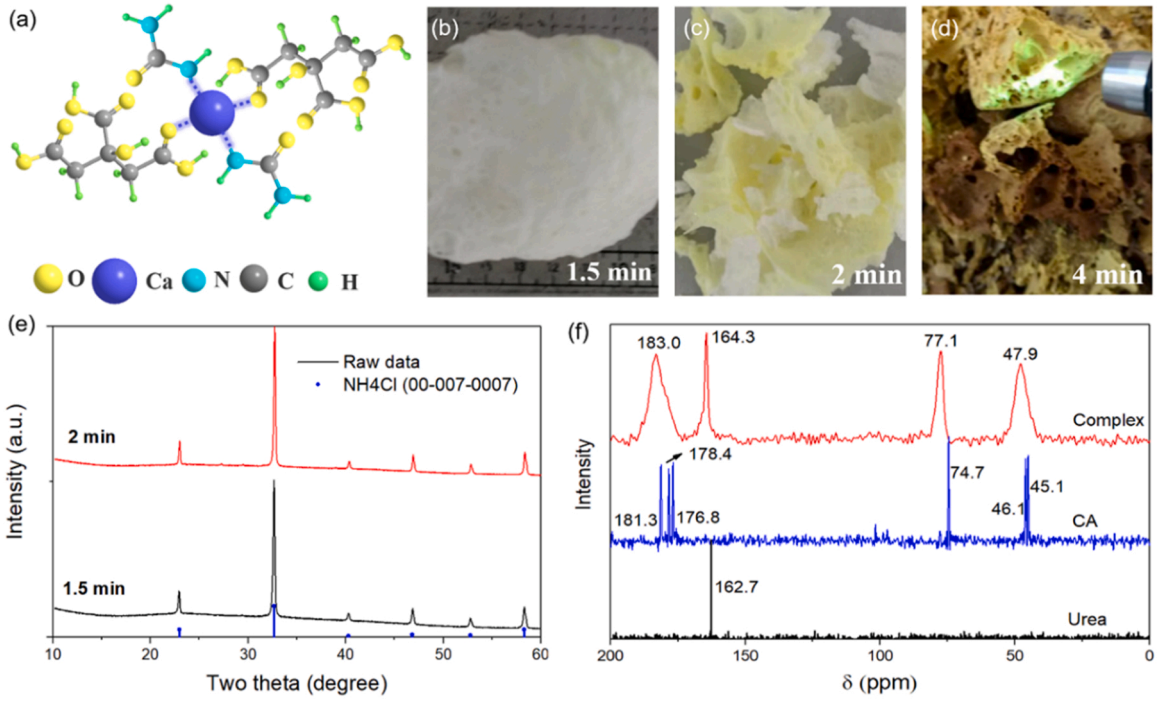

Fig. 1. (a) Structural scheme of the complex formed by microwave heating the mixture of CA/urea/$CaCl_2$ for 1.5 min (b-d) The complex obtained after (b) 1.5 min, (c) 2 min, and (d) 4 min microwave heating. (e) XRD patterns of complex after 1.5 min and 2 min heating. (e) C [13] SSNMR of the complex after 1.5 min heating, CA and urea.

the amount of the precursors. The reaction yield is around 60%, which is close to the vacuum heating reaction with a production yield of 56%, but with much shorter reaction time (4 min vs 2–3 h). X-ray powder diffraction (XRD) result of the foam formed after 1.5 min and 2 min reaction indicated that the foam-structure is mainly NH_4Cl crystal (Fig. 1e) [18]. There is no diffraction pattern of the $CaCl_2$, CA and Urea, indicating that the Ca cation reacted with the carboxyl group of the CA and formed the amorphous calcium carboxylate, similarly to the previous report [23]. The solid-state ^{13}C nuclear magnetic resonance (SSNMR) spectrum showed a typical carboxyl bond, located at 47.9, 77.1, 164.3, and 183.0 ppm, with shifting around 1.6–6.2 ppm compared to both CA (45.1, 46.1, 74.7, 176.8, 178.4, and 181.3 ppm) and urea (162.7 ppm) (Fig. 1f and Fig. S4). All the typical peaks of the complex have a broad distribution, which is due to the formation of the calcium carboxylate and Ca^{2+}-N(H_2) complex (Fig. 1e). The Fourier transform infrared (FT-IR) spectrum also indicated the newly formed bond of calcium carboxylate as the vibration from the C═O large decrease in the spectral region 1743–1689 cm^{-1} (Fig. S5). The shift of the vibration of the amine group to lower wavenumber suggested the formation of the complex between the Ca cation and urea (Fig. S5). Based on these results, we deduced that the microwave heating leads to the fast formation of the CA-Ca-urea complex (as shown in Fig. 1a). After full evaporation of the water at 100 ℃, further increasing temperature leads to the reaction between the CA and the $CaCl_2$, forming Ca (CA) and intermediate product of HCl. HCl further reacted with urea and released CO_2 and formation of NH_4Cl. With the fast increase of temperature from 100 to 160 ℃, the fast formation and evaporation of the CO_2 in less than 10 s contributed to the formation of foam structure even without the vacuum pump [8,18,23]. Further increasing the heating time, we found large amount of moisture and strong odors, which usually derive from the dehydration and deamination when the temperature is above 200 ℃. In summary, the fast reaction rate and the formation of CO_2 enable the stable foam structure consisting of CA-metal-urea complex even without vacuum pumping, giving an efficient and fast approach for high-quality C-dots synthesis.

Benefiting from the foam structure, the as-prepared C-dots have a uniform size distribution with good crystalline structure, as shown in their transmission electron microscopy (TEM) images (Fig. 2a-d and Fig. S6-8). The measured *d*-spacing based on the high-resolution TEM (HRTEM) image is around 0.24 nm and 0.21 nm, corresponding to the (100) and (112) lattice spacing of graphitic carbon [25]. With the increase of the reaction time from 2 min to 4 min, the size of the C-dots increases from (3.2 ± 0.7) to (4.0 ± 0.9) nm (Fig. S6). The X-ray photoelectron spectroscopy showed that the purified C-dots mainly contained C, N and O, with low amount of Ca [3.7% for C-dots (2 M) and 0.5% for C-dots (4 M)], which is probably bonded on the surface of the C-dots through (C═O)Ca (Fig. 2e). The C 1s spectrum of the purified C-dots indicates three components located at 284.8, 285.8, and 289.1 eV, assigned to C-C/C═C, C-N/C-O and C═O, as shown in Fig. 2f. The N 1s spectrum of C-dots (2 M) was fitted with two components of pyridinic/pyrrole N located at 399.6 eV, and graphitic N centered at 400.5 eV (Fig. 2g). The C-dots (4 M) have carbon content of 83%, which is higher than 59% of C-dots (2 M). Meanwhile, the C-dots (4 M) have only 4% of N, much less than 13% of C-dots (2 M). XPS and TEM results indicated that the C-dots (4 M) have a highly crystalline core, mainly consisting of carbon with less surface functional groups compared to the C-dots (2 M).

3.2. *Optical properties of the C-dots*

The as-prepared C-dots showed a typical absorption ranging from 200–500 nm with a first excitonic absorption peak located at 406 nm. With the increase of the reaction time, the absorption peak centered at 330 nm became lower and the peak centered at 406 nm became stronger, indicating that the intermedium molecular-like structure gradually transformed to highly carbonization core. Differently from the long-wavelength absorption ranging from 500–600 nm in C-dots produced by CA and urea (Fig. 3a), the C-dots synthesized using metal cations do not have long-wavelength absorption tail (Fig. S9). For the C-dots (2 M), the PL peaks gradually shifted to the longer wavelength, showing a typical excitation-dependent behavior (Fig. 3b). For example, as shown in Fig. S10, we can see blue and green color of the solution upon

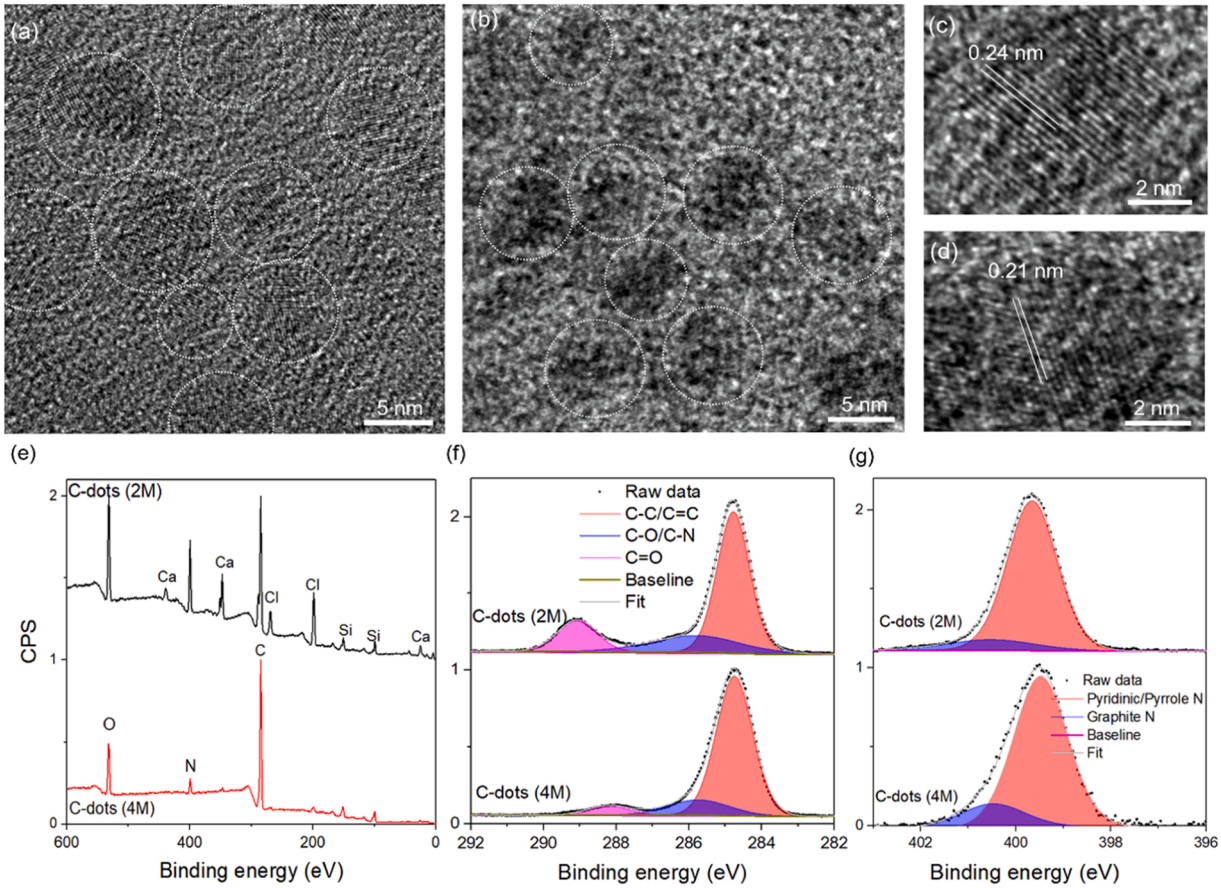

Fig. 2. TEM images of the (a) C-dots (2 M) and (b) C-dots (4 M). HRTEM images of the (c) C-dots (2 M) and (d) C-dots (4 M). (e) XPS survey spectra of the as-purified C-dots. High resolution XPS spectra of (f) C 1 s and (g) N 1s of the C-dots (2 M) and C-dots (4 M).

illumination at 365 nm and 395 nm. In a big contrast, there is no such PL behavior for the C-dots with longer time or two-step approach (Fig. 3b and Fig. S11). In fact, C-dots produced by NaCl, and $SrCl_2$ also showed an excitation dependent PL behavior (Fig. S12), compared to other metal chloride ($AlCl_3$, $MgCl_2$, $BaCl_2$, $MnCl_2$). Compared to the system with the addition of metal cations, the C-dots produced by CA/urea have a broader PL peak (Fig. S1c), due to the uncontrollable reaction process deriving from the high precursors concentration in the solid-state.

The QYs and lifetimes of the purified C-dots were measured. We found that all the samples have a typical lifetime ranging from 10.2 to 12.6 ns (Fig. 3d and Fig. S1d). The measured QYs are 15% and 73% for the C-dots (2 M) and C-dots (4 M), respectively (Fig. 3e, f and Fig. S13a). The use of the Ca cation gives the highest QY (73%) among other types of the cations or without cation (Fig. 3f). In addition, this value is also higher than the QY (50%) of the C-dots synthesized using CA/urea/$CaCl_2$ with mass ratio of 1:2:1 (Fig. S13b). The different QYs in the C-dots synthesized using different cations might be due to the following two reasons: (i) The cation induced different foam structure, which could lead to different size/size distribution of the C-dots; (ii) The cation can interact with the surface carboxyl group and form a stable surface structure, improving the surface passivation [8]. We further characterized the photostability of the C-dots (4 M), which maintained 80% of its initial value after 10-h illumination (Fig. S14), proving the C-dots having good photostability.

Ultra-fast femtoseconds transient absorption spectroscopy (fs-TAS) was used to monitor the exciton dynamic in C-dots (4 M). The excitation wavelength was set at 365 nm and the probe ranging from 400–800 nm with the resolution of 150 fs. As shown in Fig. 4a, b, a clear negative peak was found after 0.16 ps, which is assigned to the simulated emission (SE) as the peak position and peak shape was similar with the PL emission [8,16,26]. Meanwhile, a broad and low intensity peak located in the range from 650 nm to 750 nm with a decay time of several picosecond is due to the excited state absorption (ESA) (Fig. 4a, b) [27]. With increase of the decay time from 164 fs to 300 ps, a continuous shift of the SE appears (Fig. 4b), indicating the variation of the energy states for the electron- hole recombination. Finally, the SE peak can settle in the 520–550 nm (Fig. 4b). Based on the static and transient absorption data, we deduced the energy diagram for the C-dots as shown in Fig. 4c. A stable interband energy level was formed in the C-dots and this energy level governs the large Stokes shift (0.65 eV) in C-dots. Meanwhile, the low intensity ESA signal, compared to strong SE explains the high QY in C-dots (4 M). Because of the stable interband energy between the highest occupied molecular orbital (HOMO) and lowest unoccupied molecular orbital (LOMO), the C-dots (4 M) also exhibited a typical excitation-independent behavior.

3.3. *Solid-state optical devices based on C-dots*

As shown in Fig. 5a, the as-fabricated LSC show a very high transmittance in the visible range. The letters of “luminescent solar concentrators” on the bottom of the LSC can be clearly seen. Upon illuminating using solar simulator, we can clearly see the concentrated green light at the edges of the LSC, indicating the concentration effect. The solid-state C-dots embedded in PVP polymer show a similar QY compared to the C-dots dispersed in ethanol, indicating that the fabrication process does not affect the quality of the C-dots. For the large-sized LSC (225 cm^2, G factor of 4.7), the LSC based on C-dots (4 M) exhibited an external optical efficiency of 3.0% and a PCE as high as 1.3%, which is comparable to the reported large-scale LSCs based on C-dots (details shown in the S. I., table S1) [8,28–30]. This high value is benefited from the high QY and

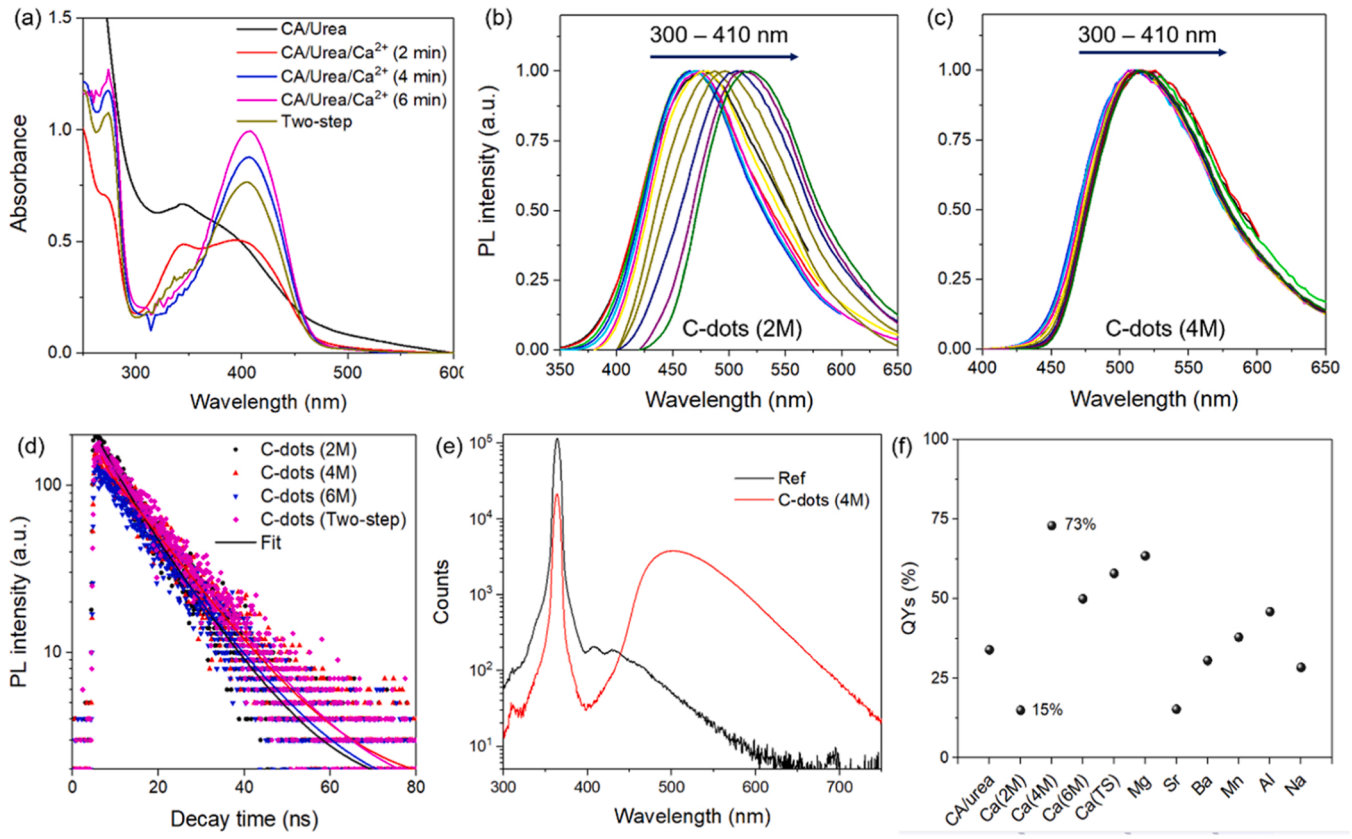

Fig. 3. (a) Absorption spectra of the C-dots synthesized via different recipes; (b-c) PL spectra of the (b) C-dots (2 M) and (c) C-dots (4 M) upon excitation at different wavelengths. (d) Fluorescence decay curves of the C-dots (4 M). The C-dots were excited at 365 nm. (e) QY of the C-dots (4 M). The C-dots were excited at 365 nm. (f) QY of C-dots synthesized at different conditions with tunable heating time (2–6 min).

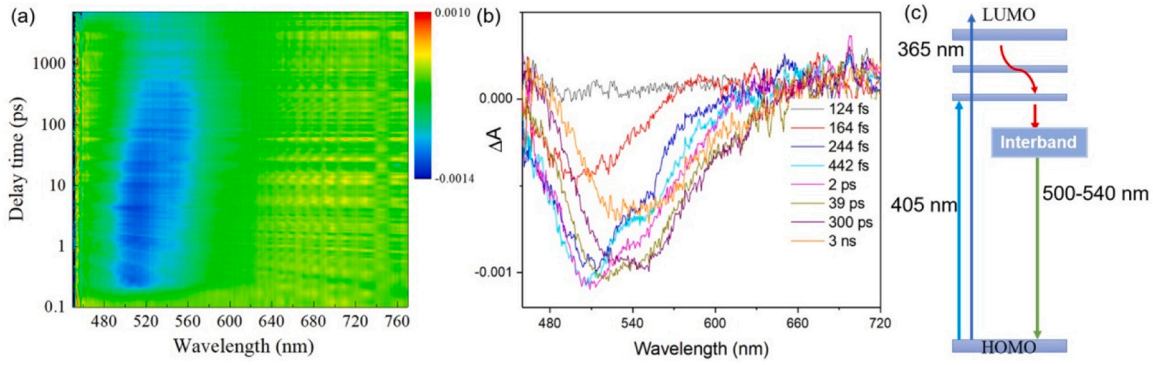

Fig. 4. (a) TA map of the C-dots (4 M); (b) TA spectra of the C-dots (4 M). λ_{ex} = 365 nm. (c) Energy diagram of the C-dots (4 M) based on static and transient absorption.

large Stokes shift of the C-dots, which prohibited the energy loss due to the reabsorption, as evidenced by the very small PL spectrum variation with the increase of the LSC length (Fig. S15). Furthermore, the as-fabricated LSC have a very good photostability. We directly measured the integrated PL area by using a PL spectrometer. It maintained 83% of its initial PL area after 40-h continuous illumination (365 nm, 100 mW/cm^2). The decrease of the PL might be due to the photo-activated surface functional groups, which induced the surface traps. Together with the low-cost and simple preparation process, the as-prepared C-dots hold a great potential for LSCs application.

These excellent optical properties of the C-dots (4 M) are also very useful as building blocks for making solid-state fluorescent security code by combination with excitation-dependent C-dots (2 M), in which we can triggered the shape and color of the code by tuning the excitation wavelength. As shown in Fig. 5e, we designed a code including the feature of the earth, LSC and leaf. The earth and LSC were printed using the C-dots (2 M) based ink and the leaf was printed using the C-dots (4 M) based ink. The fluorescent inks for the printing were shown in Fig. S10. Under room light, we cannot identify the shape of the code. While upon illumination at 365 nm, we can clearly see the shape and color of the images. The earth shows the blue color and the leaf and LSC show the green color. By shifting the excitation to 395 nm, we found the earth show the green color, similar with those of LSC and leaf. Benefiting from the high brightness and excitation dependent behavior of the C-dots, we can achieve the printed pattern with clear lines and high precision, showing a great potential for the anticounterfeiting applications

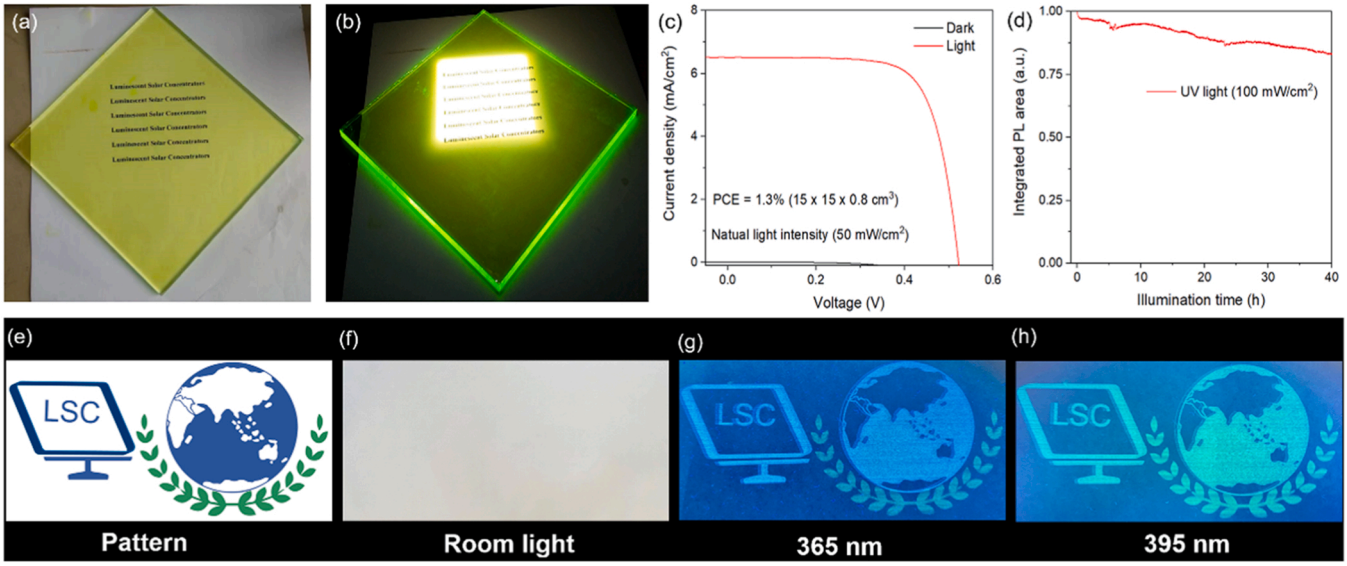

Fig. 5. (a-b) An LSC with dimension of 225 cm^2 under (a) room light or (b) simulated sunlight. (c) J-V curve of the C-dots based LSC. (d) Integrated PL area as a function of illumination time (365 nm, 100 mW/cm^2). (e) Pattern. (f) The printed pattern on flexible paper under room light. (g-h) Fluorescent code of the pattern under 365 and 395 nm UV light.

[18,31].

4. Conclusions

In summary, we demonstrated a simple and efficient microwave-assisted heating approach to produce large-scalable C-dots with very high QY (73%) and large Stokes shift (0.65 eV). The formation of the carboxyl-metal-amine complex contributed to the formation of the foam-structure, enabling the spatial confined growth of the C-dots with designed structure. The transient PL and absorption spectroscopy revealed the exciton dynamic and explains the structure-dependent optical behaviors of the C-dots. The highly crystalline core structure, together with the well passivated surface by metal cation contributed to the high QY and large Stokes shift. As a proof-of-concept, we demonstrated a highly efficient LSC with an optical efficiency of 3.0% and a PCE of 1.3% (225 cm^2) upon natural sunlight (50 mW/cm^2). By combination of excitation dependent or independent PL of the C-dots, we produced high security-level bright fluorescent code for anticounterfeiting. These results indicate that the high-quality C-dots hold a great potential for solid-state optical devices and other applications linked to their outstanding optoelectronic properties.

CRediT authorship contribution statement

Meng Xiangyong: Investigation, Formal analysis, Data curation. **Lin Jishuai:** Methodology, Formal analysis, Data curation. **Wang Maorong:** Methodology, Investigation, Formal analysis, Conceptualization. **Wang Lihua:** Methodology, Investigation, Data curation. **Zhao Haiguang:** Writing – review & editing, Supervision, Resources, Conceptualization. **Vomiero Alberto:** Writing – review & editing, Validation, Supervision. **Wang Xiaohan:** Writing – original draft, Methodology, Formal analysis, Data curation, Conceptualization. **Li Weihua:** Writing – original draft, Formal analysis, Data curation. **Song Yang:** Writing – review & editing, Supervision, Methodology, Conceptualization. **Jing Qiang:** Investigation, Formal analysis, Data curation.

Declaration of Competing Interest

The authors declare that they have no known competing financial interests or personal relationships that could have appeared to influence the work reported in this paper.

Data Availability

Data will be made available on request.

Acknowledgements

H. Zhao thanks Shandong Natural Science Funds for Distinguished Young Scholar (Nos. ZR2020JQ20) and Youth Innovation Team Project of Shandong Provincial Education Department. X.H Wang thanks Shandong Natural Science Funds (ZR2022EQ036). A. Vomiero acknowledges the Kempe Foundation, the Wallenberg Foundation, the Vetenskapsrädet under contract 2022–05024 and the Italian MUR under PNRR NEST program for financial support.

Appendix A. Supporting information

Supplementary data associated with this article can be found in the online version at doi:10.1016/j.nanoen.2024.109289.

References

[1] J. Bao, M.G. Bawendi, A colloidal quantum dot spectrometer, Nature 523 (2015) 67–70.
[2] H. Ding, S.-B. Yu, J.-S. Wei, H.-M. Xiong, Full-color light-emitting carbon dots with a surface-state-controlled luminescence mechanism, ACS Nano 10 (2016) 484–491.
[3] W. Meng, X. Bai, B. Wang, Z. Liu, S. Lu, B. Yang, Biomass-derived carbon dots and their applications, Energy Environ. Mater. 2 (2019) 172–192.
[4] C. Xia, S. Zhu, T. Feng, M. Yang, B. Yang, Evolution and synthesis of carbon dots: from carbon dots to carbonized polymer dots, Adv. Sci. 6 (2019) 1901316.
[5] Y. Liu, N. Xiao, N. Gong, H. Wang, X. Shi, W. Gu, L. Ye, One-step microwave-assisted polyol synthesis of green luminescent carbon dots as optical nanoprobes, Carbon 68 (2014) 258–264.
[6] F. Yuan, Z. Wang, X. Li, Y. Li, Za Tan, L. Fan, S. Yang, Bright Multicolor Bandgap Fluorescent Carbon Quantum Dots for Electroluminescent Light-Emitting Diodes 29 (2017) 1604436.
[7] A. Xu, G. Wang, Y. Li, H. Dong, S. Yang, P. He, G. Ding, Carbon-based quantum dots with solid-state photoluminescent: mechanism, implementation, and application, Adv. Mater. 16 (2020) 2004621.
[8] H. Zhao, G. Liu, S. You, F.V.A. Camargo, M. Zavelani-Rossi, X. Wang, C. Sun, B. Liu, Y. Zhang, G. Han, A. Vomiero, X. Gong, Gram-scale synthesis of carbon quantum dots with a large Stokes shift for the fabrication of eco-friendly and high-efficiency luminescent solar concentrators, Energ. Environ. Sci. 14 (2021) 396–406.
[9] J. Wang, J. Zheng, Y. Yang, X. Liu, J. Qiu, Y. Tian, Tunable full-color solid-state fluorescent carbon dots for light emitting diodes, Carbon 190 (2022) 22–31.
[10] J. Guo, Y. Li, X. Shan, D. Wang, P. Tian, Y. Wang, Facile microwave synthesis of efficient green emissive carbon dots powder and their application in visible light

communication and white light emitting devices, Adv. Opt. Mater. 11 (2023) 2300984.
[11] A. Karagianni, N.G. Tsierkezos, M. Prato, M. Terrones, K.V. Kordatos, Application of carbon-based quantum dots in photodynamic therapy, Carbon 203 (2023) 273–310.
[12] G. Liu, M. Zavelani-Rossi, G. Han, H. Zhao, A. Vomiero, Red-emissive carbon quantum dots enable high efficiency luminescent solar concentrators, J. Mater. Chem. A 11 (2023) 8950–8960.
[13] T. Yuan, F. Yuan, L. Sui, Y. Zhang, Y. Li, X. Li, Za Tan, L. Fan, Carbon quantum dots with near-unity quantum yield bandgap emission for electroluminescent light-emitting diodes, Angew. Chem. Int. Ed. 62 (2023) e202218568.
[14] B. Wang, G.I.N. Waterhouse, S. Lu, Carbon dots: mysterious past, vibrant present, and expansive future, Trends Chem. 5 (2023) 76–87.
[15] M. Fang, B. Wang, X. Qu, S. Li, J. Huang, J. Li, S. Lu, N. Zhou, State-of-the-art of biomass-derived carbon dots: Preparation, properties, and applications, Chin. Chem. Lett. 35 (2024) 108423.
[16] F. Yuan, T. Yuan, L. Sui, Z. Wang, Z. Xi, Y. Li, X. Li, L. Fan, Za Tan, A. Chen, M. Jin, S. Yang, Engineering triangular carbon quantum dots with unprecedented narrow bandwidth emission for multicolored LEDs, Nat. Commun. 9 (2018) 2249.
[17] Z. Yang, M. Gao, W. Wu, X. Yang, X.W. Sun, J. Zhang, H.-C. Wang, R.-S. Liu, C.-Y. Han, H. Yang, W. Li, Recent advances in quantum dot-based light-emitting devices: Challenges and possible solutions, Mate. Today 24 (2019) 69–93.
[18] S. Ren, B. Liu, G. Han, H. Zhao, Y. Zhang, Surface chemistry in calcium capped carbon quantum dots, Nanoscale 13 (2021) 12149–12156.
[19] J. Wang, Q. Li, J. Zheng, Y. Yang, X. Liu, B. Xu, N, B-codoping induces high-efficiency solid-state fluorescence and dual emission of yellow/orange carbon dots, ACS Sustain Chem. Eng. 9 (2021) 2224–2236.
[20] J.-Y. Wei, Q. Lou, J.-H. Zang, Z.-Y. Liu, Y.-L. Ye, C.-L. Shen, W.-B. Zhao, L. Dong, C.-X. Shan, Scalable synthesis of green fluorescent carbon dot powders with unprecedented efficiency, Adv. Opt. Mater. 8 (2020) 1901938.
[21] K. Jiang, Y. Wang, X. Gao, C. Cai, H. Lin, Facile, quick, and gram-scale synthesis of ultralong-lifetime room-temperature-phosphorescent carbon dots by microwave irradiation, Angew. Chem. Int. Ed. 57 (2018) 6216–6220.
[22] Y. Zhang, X. Liu, Y. Fan, X. Guo, L. Zhou, Y. Lv, J. Lin, One-step microwave synthesis of N-doped hydroxyl-functionalized carbon dots with ultra-high fluorescence quantum yields, Nanoscale 8 (2016) 15281–15287.
[23] D. Zhou, P. Jing, Y. Wang, Y. Zhai, D. Li, Y. Xiong, A.V. Baranov, S. Qu, A. L. Rogach, Carbon dots produced via space-confined vacuum heating: maintaining efficient luminescence in both dispersed and aggregated states, Nanoscale Horiz. 4 (2019) 388–395.
[24] A. Macina, T.V. de Medeiros, R. Naccache, A carbon dot-catalyzed transesterification reaction for the production of biodiesel, J. Mater. Chem. A 7 (2019) 23794–23802.
[25] L. Tang, L. Ai, Z. Song, L. Sui, J. Yu, X. Yang, H. Song, B. Zhang, Y. Hu, Y. Zhang, Y. Tian, S. Lu, Acid-triggered aggregation of carbon dots shifted their emission to give unexpected deep-red lasing, Adv. Funct. Mater. 33 (2023) 2303363.
[26] S. Mondal, A. Yucknovsky, K. Akulov, N. Ghorai, T. Schwartz, H.N. Ghosh, N. Amdursky, Efficient photosensitizing capabilities and ultrafast carrier dynamics of doped carbon dots, J. Am. Chem. Soc. 141 (2019) 15413–15422.
[27] B. Wang, Z. Wei, L. Sui, J. Yu, B. Zhang, X. Wang, S. Feng, H. Song, X. Yong, Y. Tian, B. Yang, S. Lu, Electron–phonon coupling-assisted universal red luminescence of o-phenylenediamine-based carbon dots, Light-Sci. Appl. 11 (2022) 172.
[28] K. Wu, H. Li, V.I. Klimov, Tandem luminescent solar concentrators based on engineered quantum dots, Nat. Photonics 12 (2018) 105–110.
[29] M. Wei, F.P.G. de Arquer, G. Walters, Z. Yang, L.N. Quan, Y. Kim, R. Sabatini, R. Quintero-Bermudez, L. Gao, J.Z. Fan, F. Fan, A. Gold-Parker, M.F. Toney, E. H. Sargent, Ultrafast narrowband exciton routing within layered perovskite nanoplatelets enables low-loss luminescent solar concentrators, Nat. Energy 4 (2019) 197–205.
[30] Y. Zhou, D. Benetti, Z. Fan, H. Zhao, D. Ma, A.O. Govorov, A. Vomiero, F. Rosei, Near infrared, highly efficient luminescent solar concentrators, Adv. Energy Mater. 6 (2016) 1501913.
[31] X. Wang, Y. Han, W. Li, J. Li, S. Ren, M. Wang, G. Han, J. Yu, Y. Zhang, H. Zhao, Doped carbon dots enable highly efficient multiple-color room temperature phosphorescence, Adv. Opt. Mater. (2023) 2301962.

Weihua Li received her Bachelor's degree in 2017 and Master's degree in 2020 from Qingdao University. She is presently a PhD candidate under the supervision of Prof. Haiguang Zhao at Qingdao University, China. Her research mainly focuses on the synthesis and structural characterization of carbon quantum dots and their application in flexible anti-counterfeiting.

Xiaohan Wang received her PhD degree in Textile Science and Engineering from Qingdao University in 2021. Currently he is an assistant professor at the State Key Laboratory, Qingdao University. Her research mainly focuses on functional nanofibers/quantum dots hybrid materials for electrocatalysis and photocatalysis.

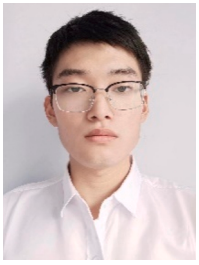

Jishuai Lin received his Bachelor's degree in School of Mechanics and Optoelectronic Physics from Anhui University of Science and Technology in 2021. Currently, he is a Master student majored in Physics at Qingdao University. His research mainly focuses on the synthesis and structural characterization of carbon quantum dots and fabrication of luminescent solar concentrators and LEDs.

Xiangyong Meng received his Bachelor degree in Engineering of inorganic non-metallic materials from Chaohu University (China) in 2022. Currently, he is a Master student majored in Materials Engineering at Qingdao University (China). His research mainly focuses on the formation mechanism and optical properties of red emitting carbon quantum dots.

Lihua Wang graduated in Applied Physics from the School of Mechanics and Photoelectric Physics, Anhui University of Science and Technology in 2021. He is currently studying as a Master student in Physics, Qingdao University, mainly engaged research in the synthesis and application of carbon quantum dots and the fabrication of luminescent solar concentrators and LEDs.

Maorong Wang received his PhD degree from Lanzhou Institute of Chemical Physics, Chinese Academy of Sciences. Currently he is a lecturer at the State Key Laboratory of Qingdao University. His research interests focus on the nuclear magnetic resonance spectroscopy, catalytic chemistry and crystallography.

Qiang Jing is an assistant Professor of College of Physics & State Key Laboratory, Qingdao University, China. He received Master degree (2015) from Harbin Institute of Technology and PhD degree (2019) from Nanjing University. His research interests focus on the synthesis of low-dimensional semiconductor materials (including quantum dots, perovskite nanocrystals and carbon quantum dots) for luminescent solar concentrator and LEDs.

Yang Song is an associate professor in Condensed Matter Physics at the State Key Laboratory and College of Physics, Qingdao University, China. He received the bachelor's degree (2015) from Shandong University and the PhD degree (2022) from University of Science and Technology of China. His research interests focus on the synthesis of low-dimensional semiconductor materials, the modulation of novel optoelectric device (such as the LEDs and flexible sensors) and developing the advanced optoelectronic characterization techniques.

Alberto Vomiero is a chair professor in Experimental Physics at the Department of Engineering Sciences and Mathematics, Luleå University of Technology, Sweden and a professor in Industrial Engineering at the Department of Molecular Sciences and Nanosystems, Ca' Foscari University of Venice, Italy. He is leading a multidisciplinary group focusing on the development of advanced nanomaterials for energy and environmental applications, including solar cells, water splitting and photocatalysis. He is a former Marie Curie International Outgoing Fellow of the European Commission, Fellow of the Swedish Foundations, of the Royal Society of Chemistry, and several other Societies.

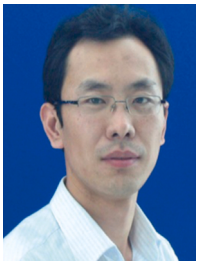

Haiguang Zhao received his BS degree (2005) from University of Jinan, M.Sc. degree (2007) from Zhejiang University and PhD degree in Energy and Materials Science (2012) from INRS, Quebec University. Currently he is a full professor at the State Key Laboratory and College of Physics, Qingdao University, since 2018. His research interests focus on quantum dots for optoelectronic applications, such as luminescent solar concentrators, thermal sensors, and solar-driven water splitting. He is a Member of the Global Young Academy.